scientific reports

OPEN

Different prefrontal cortex activity patterns in bipolar and unipolar depression during verbal fluency tasks based on functional near infrared spectroscopy study

Lan Mou[1,5], Yuqi Shen[2,5], Boyuan Wu[3], Chengyu Zhang[4], Jiayun Zhu[3], Qian Tan[2], Xiaomei Zhang[1], Zefeng Wang[3] & Zhongxia Shen [1✉]

This study aimed to investigate the functionality of the prefrontal cortex in patients with unipolar depression (UD) and bipolar depression (BD) using functional near-infrared spectroscopy (fNIRS) during a verbal fluency task (VFT). Additionally, it evaluated the reliability of fNIRS as a diagnostic tool for cognitive assessments through a deep learning approach using one-dimensional convolutional networks. The study included 73 patients with UD, 59 patients with BD, and 40 healthy controls (HC). Hemodynamic responses in the prefrontal cortex were recorded using fNIRS during the VFT. Differences in oxygenated hemoglobin concentrations across the three groups were compared, and receiver operating characteristic (ROC) curves were generated for each region of interest. Both UD and BD patients demonstrated significantly reduced activation in the prefrontal cortex compared to healthy controls. UD patients showed notably lower activation values than BD patients in the dorsolateral prefrontal cortex, frontopolar prefrontal cortex, left orbitofrontal cortex, and left ventrolateral prefrontal cortex. The highest classification accuracy (79.57%) was observed in the left orbitofrontal cortex. The UD group had the largest area under the ROC curve (AUC = 0.99) in the left orbitofrontal cortex, while the BD group had the largest AUC (0.91) in the right dorsolateral prefrontal cortex. The HC group exhibited the largest AUC (0.73) in the same region. The DLPFC, FPC, lOFC, and lVLPFC may serve as biomarker regions for differentiating UD from BD. The combination of fNIRS and the VFT shows promise as a supplementary diagnostic tool for mental health disorders.

Keywords Bipolar disorder, Unipolar depression, FNIRS, Verbal fluency task

Bipolar disorder (BD) is a chronic, recurrent condition primarily characterized by fluctuations in mood and energy levels[1,2]. Depression often presents as the initial symptom, accounting for approximately 75% of symptomatic episodes[3]. The severity and nature of bipolar depression often resemble those of unipolar depression (UD)[3–5]. Notably, around 69% of individuals with BD are initially misdiagnosed with UD. On average, patients consult four different doctors before receiving an accurate diagnosis of BD, which poses significant challenges for both patients and their families[6]. In the first five years after a UD diagnosis, the conversion rate to BD is approximately 2.5% annually, dropping to 0.5% per year thereafter[7]. Consequently, this study focuses on UD patients with a history of recurrent depressive episodes lasting more than five years. The annual suicide rate among BD patients is approximately 0.9%, compared to just 0.014% in the general population, and an estimated 15–20% of individuals with BD die by suicide. This underscores the need for early diagnosis and treatment to improve patient outcomes[3].

[1]Sleep Medical Center of Huzhou Third Municipal Hospital, the Affiliated Hospital of Huzhou University, Huzhou 313000, People's Republic of China. [2]School of Mental Health, Wenzhou Medical University, Wenzhou 325000, People's Republic of China. [3]School of Information Engineering, Huzhou University, Huzhou 313000, People's Republic of China. [4]Department of Psychosis Studies, Institute of Psychiatry Psychology & Neuroscience, King's College London, De Crespigny Park, SE5 8AF London, GB, UK. [5]Lan Mou and Yuqi Shen co-first authors. ✉email: snowszx@sina.com

Distinct pathophysiological mechanisms differentiate BD from UD, including variations in brain structure, inflammation levels, and brain function[8]. Current diagnoses for these disorders rely on the DSM-5 and ICD-10 classifications[9,10]. However, identifying objective biomarkers that reflect the inherent characteristics of these disorders is crucial for accurate differentiation between UD and BD[11].

Previous research has revealed that BD patients exhibit mitochondrial dysfunction and metabolic decline in the prefrontal cortex (PFC)[12]. A In contrast, patients with major depressive disorder (MDD) demonstrate dysregulation in prefrontal circuits, with structural and functional changes in the PFC playing a key role in mood disorders[13]. Redlich et al. found that UD patients exhibited reduced activation in both the nucleus accumbens (NAC) and the PFC compared to BD patients[14]. While functional magnetic resonance imaging (fMRI) is the predominant tool used in cognitive studies of mood disorders, it is costly, requires complex operational maintenance, and is highly sensitive to head movements, potentially compromising data quality. These limitations hinder the broader adoption of fMRI. In light of these challenges, functional near-infrared spectroscopy (fNIRS) offers a promising alternative for examining cognitive and functional brain changes in BD and UD patients[15].

The fNIRS is an optical neuroimaging technique that uses near-infrared light to track changes in concentrations of oxygenated hemoglobin (Oxy-Hb) and deoxygenated hemoglobin (Deoxy-Hb) to investigate brain function[16]. Compared to electroencephalography (EEG) or functional magnetic resonance imaging (fMRI), functional near-infrared spectroscopy (fNIRS) offers unique advantages. Its relatively portable equipment allows for use in various environments, and it is safe, non-invasive, unrestrictive, quiet, motion-tolerant, and cost-effective[17]. fNIRS has been proven effective in detecting brain function and serves as a viable alternative for patients unable to undergo fMRI. When conducting brain function assessments on individuals with BD and UD, physical movement may occur due to emotional instability or restlessness. However, fNIRS demonstrates a high tolerance to motion artifacts. Additionally, given the psychologically sensitive and vulnerable nature of BD and UD patients, fNIRS only requires probe placement on the scalp surface, avoiding discomfort or potential risks.fNIRS is particularly effective in measuring oxygenation changes in the prefrontal cortex during cognitive tasks[18] a region critical for cognitive control[19]. The prefrontal cortex is closely associated with stress perception, emotional regulation, and executive function[20]. Executive function refers to the ability to plan, make decisions, and self-regulate in the face of complex tasks[21]. Cognitive impairments, especially those affecting executive function, are commonly observed in BD and MDD[22,23].

Among emotional and cognitive tasks, the verbal fluency task (VFT) is widely considered one of the most effective measures for assessing the control, planning, activation, and monitoring processes involved in emotional regulation[24]. During the VFT, participants are asked to generate as many unique words as possible within given categories (phonemic or semantic) under time constraints[25]. This task requires the initiation of verbal behaviors, strategic retrieval of verbal information, and self-monitoring to avoid intrusions and repetitions[26]. The VFT has been extensively used in fNIRS research to explore functional cognitive impairments.

Despite the growing body of research on BD and UD, few studies have examined brain activation patterns in these patients during fNIRS-VFT tasks. One study observed that BD patients exhibited decreased activation in the bilateral ventrolateral prefrontal cortex and anterior temporal cortex compared to healthy controls[27]. Additionally, Feng et al. found that BD patients showed lower activation in the left inferior frontal gyrus during the VFT, while UD patients demonstrated reduced activation in the left dorsolateral prefrontal cortex, bilateral ventrolateral prefrontal cortex, and bilateral orbitofrontal cortex[15]. Although these studies relied heavily on manual feature extraction, recent advancements in deep learning offer more efficient and accurate approaches. To improve the differentiation between BD and UD, this study applies a supervised learning approach using a one-dimensional convolutional neural network (1D-CNN), which captures temporal fluctuations in emotional states[28]. By extracting key features associated with emotional disorders, our model enhances the accuracy of distinguishing BD from UD[29] thereby providing a more robust foundation for clinical diagnosis.
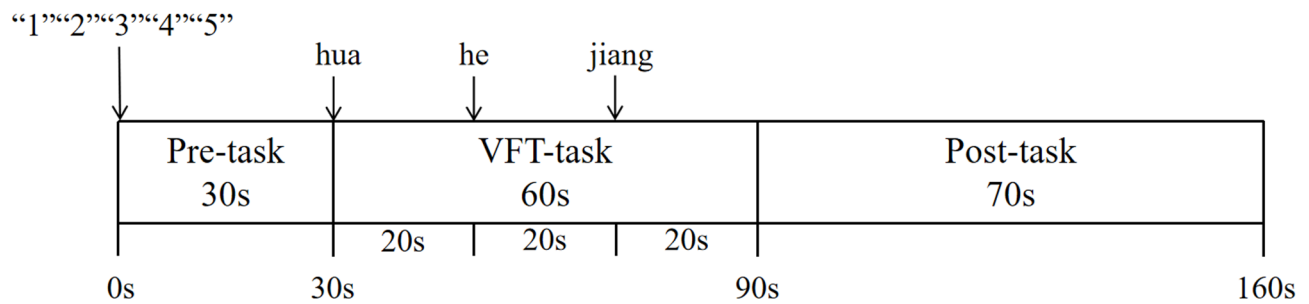
We therefore hypothesized that abnormalities in prefrontal area functioning may lead to enhanced negative emotions in BD and UD, and that abnormal activation in patients with BD may be emotional state specific, with activation showing a biphasic dynamic imbalance.This study utilizes fNIRS to investigate prefrontal cortex activation in UD and BD patients, as well as healthy controls, during a verbal fluency task. By integrating deep learning techniques with 1D-CNN analysis, we aim to identify specific brain regions or activation patterns that can differentiate between UD and BD, providing a more objective foundation for clinical diagnosis.
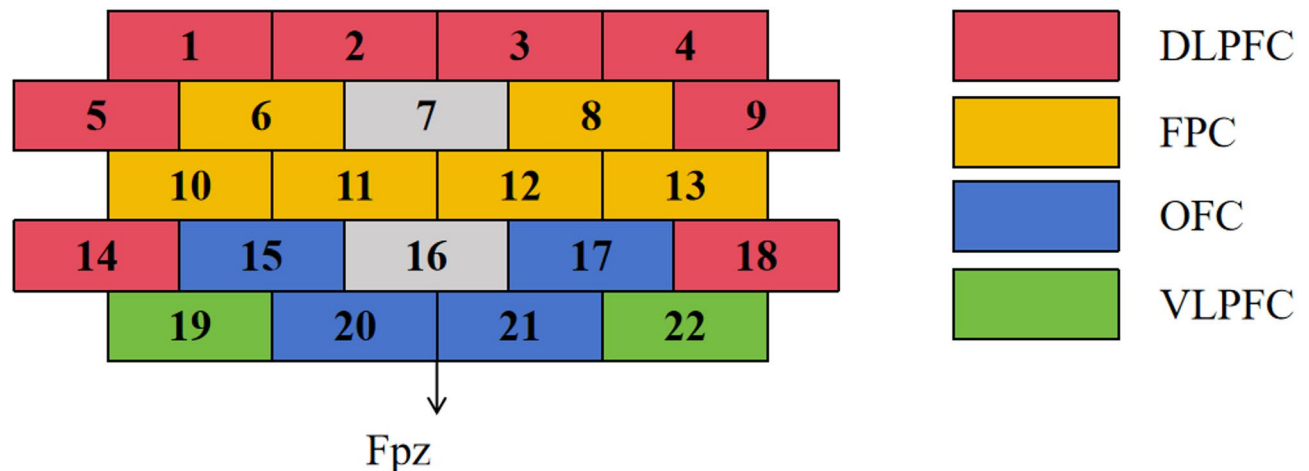
Materials and methods
Participants
This study included 172 patients treated at Huzhou Third People's Hospital between November 2022 and August 2024. The inclusion criteria were as follows: (1) meeting diagnostic criteria for bipolar disorder with depressive episodes or recurrent depressive disorder according to the Diagnostic and Statistical Manual of Mental Disorders, Fifth Edition (DSM-5), confirmed by two psychiatrists; (2) age range of 18 to 60; (3) a Hamilton Depression Rating Scale (HAMD-17) score above 17; (4) a Young Mania Rating Scale (YMRS) score below 7; (5) right-handedness; and (6) at least a primary education level. Exclusion criteria included: (1) presence of other psychiatric disorders, such as schizophrenia or dementia; (2) a significant medical history; (3) recent receipt (within the past month) of electroconvulsive therapy (MECT) or repetitive transcranial magnetic stimulation (rTMS); (4) history of substance or alcohol abuse; (5) diagnosis of a first depressive episode; and (6) pregnancy or breastfeeding. Additionally, 40 healthy controls (HC) matched for gender, age, and education level were recruited, with HAMD-17 scores below 7.

This study was approved by the ethical review committee of Huzhou Third People's Hospital, and informed consent was obtained from all participants prior to inclusion.

Fig. 1. Verbal fluency task.

Fig. 2. Distribution of fNIRS channels and corresponding brain regions.

Verbal fluency task

The verbal fluency task (VFT) is designed to assess vocabulary knowledge, linguistic creativity, and executive function[30]. The test consists of three phases: a 30-second preparation rest period, a 60-second formal task period, and a 70-second recovery rest period. During the preparation and recovery phases, participants are instructed to verbally repeat the numbers one through five. In the formal task phase, participants are prompted to generate as many words as possible using the Chinese characters "hua," "he," and "jiang," with a 20-second time limit per character. Participants remain seated and minimize movements throughout the test to ensure accuracy of the results (Fig. 1).

fNIRS measurement

In this study, we used the ETG-ONE functional near-infrared spectroscopy (fNIRS) imaging device from Hitachi, Japan, to measure brain activity. This device operates by emitting near-infrared light at wavelengths of 695 nm and 830 nm. We configured 22 channels, consisting of 8 emitter probes and 7 receiver probes, arranged in a 3×5 layout over the frontal lobe region. The distance between each emitter and receiver probe was set to 3 centimeters, with measurement points positioned 2–3 centimeters subcutaneously, corresponding to the cortical surface[31] at a sampling rate of 10 Hz. Probe placement followed the EEG 10–20 system, initially positioning the central probe of the bottom row at the brow ridge and extending the remaining channels from the brow ridge to the pinna. Based on Brodmann area distributions, channels were assigned to specific prefrontal regions: the dorsolateral prefrontal cortex (DLPFC) included channels 1, 2, 3, 4, 5, 9, 14, and 18; the frontopolar prefrontal cortex (FPC) included channels 6, 8, 10, 11, 12, and 13; the orbitofrontal cortex (OFC) included channels 15, 17, 20, and 21; and the ventrolateral prefrontal cortex (VLPFC) included channels 19 and 22 (Fig. 2). Cortical activation was recorded during the verbal fluency task, and concentrations of oxygenated and deoxygenated hemoglobin in the cortex were indirectly calculated along with their differential concentrations, based on the Beer-Lambert law.

Data analysis

Data analysis was conducted using SPSS 26.0 and MATLAB. Quality control of the fNIRS data was performed using the NIRS_KIT toolbox (MATLAB 2021a)[32] to check for physiological noise, time-domain, frequency-domain, or spatial features of head motion artefacts. Preprocessing was then initiated. The initial preprocessing step involved detrending the raw data. Motion artifacts were then corrected using the TDDR method, followed

by the application of a third-order IIR Butterworth bandpass filter (0.001 to 0.1 Hz) to remove irrelevant low- and high-frequency components. After filtering, optical data signals detected by the photodetectors were converted into oxygenated hemoglobin (Oxy-Hb) and deoxygenated hemoglobin (deoxy-Hb) concentrations using an enhanced Beer-Lambert law. Only Oxy-Hb was analyzed, as prior studies suggest that Oxy-Hb more accurately reflects changes in regional cerebral blood flow compared to Deoxy-Hb[33]. the Oxy-Hb signal is a more direct reflection of cognitive activation than the Deoxy-Hb signa[34] and therefore Oxy-Hb levels have been used to compute cortical activity to analyze fNIRS data[35].

Cortical activation was indicated by increases in Oxy-Hb, calculated by subtracting the mean Oxy-Hb values during the resting periods before and after the task from the average Oxy-Hb during the task.

Data counts are reported as frequencies or percentages (%), with chi-square tests used for intergroup comparisons. The Shapiro-Wilk test was used to assess normality for quantitative data. Normally distributed data is presented as mean ± standard deviation (`x ± s) and analyzed using one-way ANOVA for intergroup comparisons. Non-normally distributed data is presented as the median and interquartile range [M(P25, P75)], with the Kruskal-Wallis rank-sum test applied for intergroup comparisons. Bonferroni correction was used for multiple comparisons. Statistical significance was set at $P < 0.05$, with a 95% confidence interval (CI) for all analyses.

Deep learning approaches

During data preprocessing, we performed data cleaning and standardization on the collected dataset. To enhance dataset diversity and robustness, we applied data augmentation techniques, including noise addition and Gaussian smoothing. We have added the following information to the revised manuscript: A combined strategy of Gaussian smoothing ($\sigma = 0.1$) and adding Gaussian noise ($\mu = 0$, $\sigma = 0.02$) was used in the data enhancement stage, and the degree of smoothing and noise intensity was controlled by adjusting the sigma parameter. The time series are dynamically truncated/filled during data loading to ensure that all samples are uniformly of preset sequence length (hyperparameters determine the specific value). The preprocessing process is completely encapsulated in the fNIRSDataset class, and the batch data loading is realized through DataLoader, which is designed to ensure the reproducibility of the experiment and the standardization of the engineering implementation. In terms of model training optimization, a dynamic adaptive hyper-parameter tuning system is constructed: the AdamW optimizer (initial learning rate 0.0002, weight decay 0.001) is used to balance the gradient updating and regularization constraints, the validation loss is monitored in real-time through the ReduceLROnPlateau scheduler, and when the loss stagnates in 5 rounds, it automatically attenuates the learning rate by 50%, and a 40-round early A 40-round early stopping mechanism is set to prevent invalid training. During the training process, a five-fold overfitting prevention and control strategy is implemented: (1) online data enhancement with randomly perturbed input signals; (2) introduction of 0.6 probability dropout at the fully connected layer; (3) built-in L2 weight constraints in the optimizer; (4) dynamic partitioning of the validation set by five-fold cross-validation; and (5) real-time termination of the overfitting tendency by early stopping mechanism. The validation system adopts a two-layer validation framework, where the outer layer divides the training set and test set by 4:1, and the inner layer refines the training set into a training subset and a validation subset by 5-fold cross-validation. Two hundred fifty rounds of iterative training are performed to ensure parameter convergence, and the final model demonstrates a stable classification performance on the independent test set. All the above experiments were conducted based on the Pytorch platform.

The model uses a three-layer one-dimensional convolutional neural network (1D-CNN) architecture. The first convolutional layer has a kernel size of 9, with 22 input channels and 64 output channels. The second layer employs a kernel size of 5, with 64 input channels and 128 output channels, and the third layer features a kernel size of 3, with 128 input channels and 256 output channels. Following each convolutional layer, we applied the ReLU activation function and batch normalization to enhance training stability. Each convolutional layer is also followed by a max pooling layer with a kernel size of 2 and a stride of 2, reducing the spatial dimensions of the feature maps.

After the 1D-CNN processes the input, we concatenated the extracted features with integral values and passed them into a fully connected layer. The first fully connected layer has an input dimension of 39,958 and an output dimension of 256, while the second layer has an input dimension of 256 and an output of 128. Each fully connected layer includes the ReLU activation function, batch normalization, and dropout to stabilize training and prevent overfitting. Finally, a Softmax function converts the output into a probability distribution corresponding to the three classes: healthy, unipolar depression, and bipolar depression.

The loss function of the model is based on cross-entropy and optimized using the AdamW algorithm with a learning rate of 0.0002 and a weight decay of 0.001. The training parameters consist of 32 batches and 250 calendar hours, with the early stopping patience set to 40 calendar hours. We used the KFold cross-validation method to divide the dataset into five folds. For each fold, the training set was randomly divided into a training subset and a validation subset. Models are trained on the training subset, losses are computed via forward propagation, and parameters are updated via backpropagation. Key performance metrics (e.g., accuracy on the validation subset) are monitored, and the learning rate is adjusted, or early stops are triggered using the ReduceLROnPlateau scheduler.

For model validation, we select 30 random seeds for experiments, and 20% of the data from each random seed is extracted as the test set, while the remaining 80% is divided into the training and validation sets by the leave-one-out method to ensure that the test set does not overlap with the training and validation sets at all. Through multiple training and validation, we calculate various performance metrics (e.g., accuracy, recall, F1 value, etc.) of the model on the training, validation, and test sets and take the average value of these metrics in order to evaluate the performance of the model on the training data more comprehensively and stably and to avoid bias in the evaluation results due to the randomness in the division of the dataset.

Diagnostic groups	UD($n = 73$)	BD($n = 59$)	HC($n = 40$)	Z/χ^2 a	p
Age (years)	50(41, 57.50)	50(37, 57)	48.5(39, 58)	0.257	0.880
Gender (F/M)	61/12	49/10	33/7	0.021	0.989
BMI	22.66(20.81,24.65)	22.86(20.03,23.73)	22.88(21.41,24.64)	1.742	0.418
Duration of illness(moth)	70(65,78)	75(66,82)	0	0.570	0.752
Education (years)	11(6.50,15)	12(6,12)	12(9,14.25)	1.853	0.173
HAMD	20(18, 22)	20(18, 22)	1(0, 2)	94.088	0.000b

Table 1. Comparison among three groups concerning demographic data and clinical scales.details. UD, unipolar depression group; BD, bipolar depression group; HC, healthy control group; BMI, body mass index; HAMD, Hamilton Depression Scale. [a]: For gender, we utilize the chi-square test, while for age, BMI, disease duration, years of education, and HAMD scores, we employ the rank-sum test. [b]: Through Bonferroni correction, post hoc comparisons indicated UD vs. HC, $p < 0.001$; BD vs. HC, $p < 0.001$; UD vs. BD, $p = 1.000$.

Region of interest	F	P	η^2_p
rDLPFC	37.205	< 0.001	0.291
lDLPFC	33.155	< 0.001	0.282
rFPC	35.122	< 0.001	0.291
lFPC	40.851	< 0.001	0.324
rOFC	42.083	< 0.001	0.340
lOFC	58.613	< 0.001	0.391
rVLPFC	37.353	< 0.001	0.306
lVLPFC	34.200	< 0.001	0.274

Table 2. Analysis of variance of changes in oxygenated hemoglobin concentration in eight brain regions in three groups.

Through multiple sets of experiments, we explored the effects of different convolutional kernel sizes (e.g., 3, 5, 7, 9, 11), step sizes (1, 2), the number of convolutional layers (1 to 5), and the number of neurons in the fully-connected layer (32, 64, 128, 256) on the effect of feature extraction and the model's ability to learn complex patterns. These experiments helped us to determine the optimal combination of parameters, which improved the overall performance of the model.

Results

Demographic and clinical characteristics

No significant gender differences were observed among the UD patients, BD patients, and healthy participants ($\chi^2 = 0.021$, $p = 0.989$), nor were there significant differences in age (Z = 0.257, $p = 0.880$), BMI (Z = 1.742, $p = 0.418$), duration of illness (Z = 0.570, $p = 0.752$), and years of education (Z = 1.853, $p = 0.173$). However, HAMD scores showed a significant difference across the three groups (Z = 94.088, $p < 0.001$) (Table 1).

Differences in prefrontal cortex activation among groups during the VFT

A one-way ANOVA was conducted on the activation values across the three groups. The results revealed significant differences in oxyhemoglobin concentration changes among the three groups across eight brain regions during the VFT (Table 2). Figure 3 presents the post-hoc comparisons across these regions, indicating a notable reduction in prefrontal cortex activation in both UD and BD patients compared to healthy participants (Fig. 3A-H). Additionally, UD patients showed significantly lower activation values than BD patients in the DLPFC, FPC, lOFC, and lVLPFC regions (Fig. 3A, B, C, D, F, H).
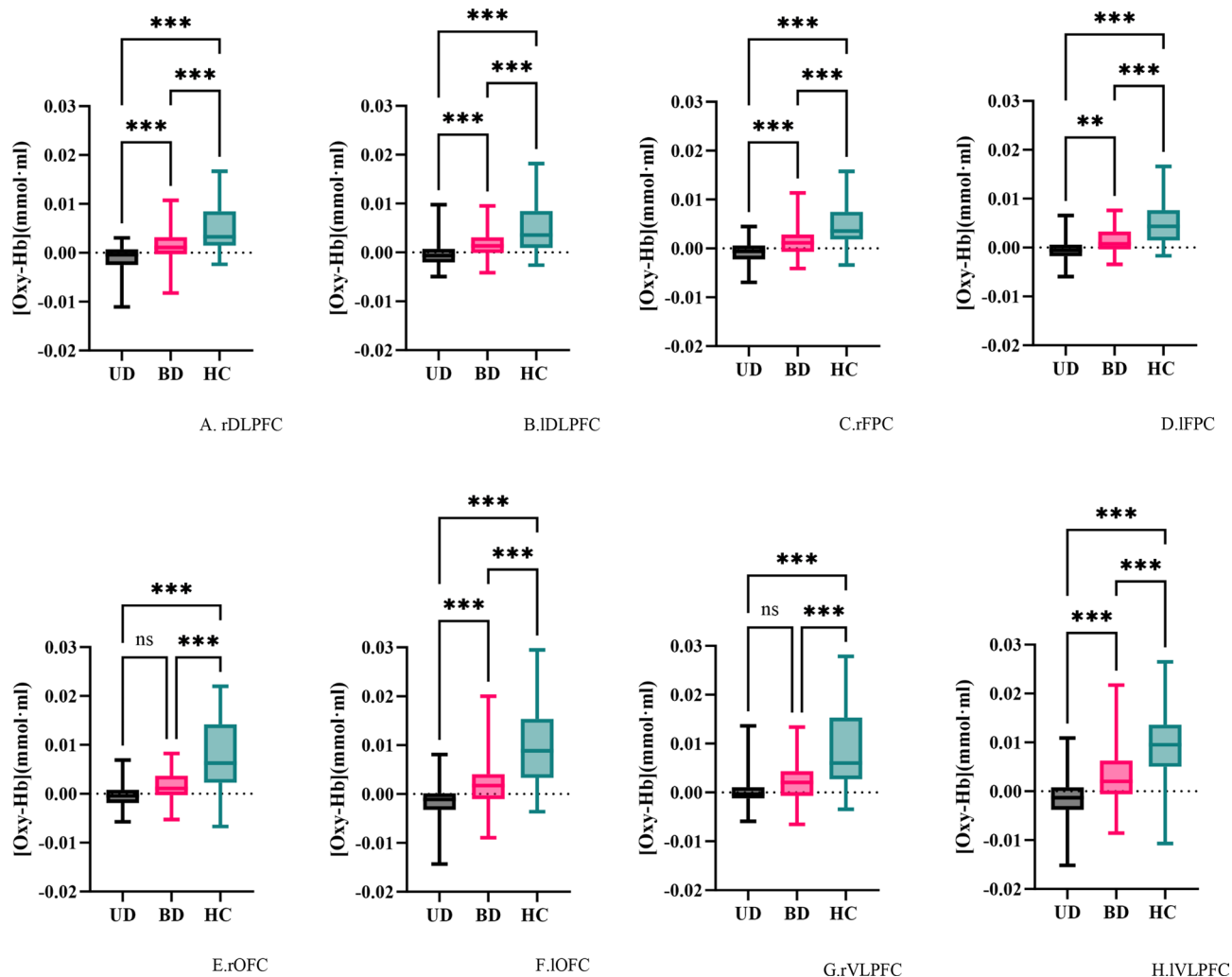
Classification (Deep Learning)

We conducted 30 randomized experiments on each brain region to assess model performance on the test set. The results, summarized in Table 3, show that the highest classification accuracy reached 79.57% in the left orbitofrontal cortex (lOFC), while the lowest accuracy was 61.64% in the left ventrolateral prefrontal cortex (lVLPFC).

Using the fNIRS classification results, we plotted the ROC curve for diagnosing UD across eight brain regions (Fig. 4). During the VFT task, the left orbitofrontal cortex (lOFC) exhibited the highest area under the curve (AUC) for UD patients, with an AUC of 0.99. The optimal cutoff value was 0.89, resulting in a sensitivity of 100% and a specificity of 89% (Table 4).

The fNIRS classification results were used to plot the ROC curve for diagnosing BD across eight brain regions (Fig. 5). During the VFT task, the right dorsolateral prefrontal cortex (rDLPFC) showed the highest area under the curve (AUC) for BD patients, with an AUC of 0.91. The optimal cutoff value was 0.66, achieving a sensitivity of 78% and a specificity of 89% (Table 5).

Fig. 3. In the task of verbal fluency, significant differences emerged in the activation of the prefrontal cortex among the three groups. (**A**) Box plots of Oxy-Hb variations in the right dorsolateral prefrontal cortex for the three groups. (**B**) Box plots of Oxy-Hb variations in the left dorsolateral prefrontal cortex for the three groups. (**C**) Box plots of Oxy-Hb variations in the right anterior prefrontal cortex for the three groups. (**D**) Box plots of Oxy-Hb variations in the left anterior prefrontal cortex for the three groups. (**E**) Box plots of Oxy-Hb variations in the right orbitofrontal cortex for the three groups. (**F**) Box plots of Oxy-Hb variations in the left orbitofrontal cortex for the three groups. (**G**) Box plots of Oxy-Hb variations in the right ventrolateral cortex for the three groups. (**H**) Box plots of Oxy-Hb variations in the left ventrolateral cortex for the three groups. (**$p < 0.01$,***$p < 0.001$).

Region of interest	Three-class classification
rDLPFC	70.00%
lDLPFC	66.97%
rFPC	72.88%
lFPC	75.34%
rOFC	76.13%
lOFC	79.57%
rVLPFC	67.56%
lVLPFC	61.41%

Table 3. The three-class classification accuracy for each brain region.
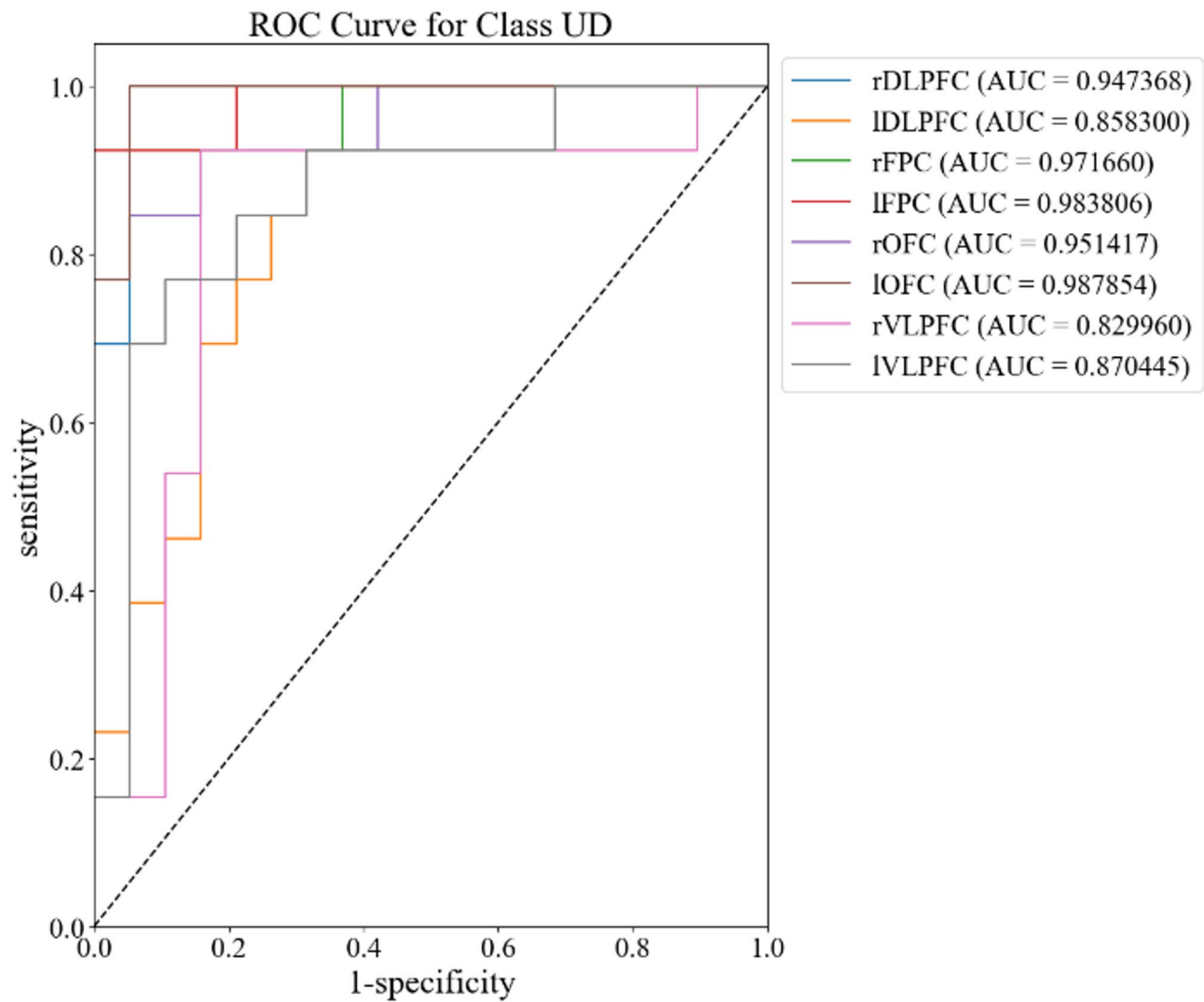
Fig. 4. ROC curve for Class UD.

Region of interest	AUC	Sensitivity	Specificity	Oxy-Hb cut-off point
rDLPFC	0.95	0.92	0.84	0.77
lDLPFC	0.86	1.00	0.63	0.63
rFPC	0.97	0.92	1.00	0.92
lFPC	0.98	0.92	1.00	0.92
rOFC	0.95	0.84	0.95	0.79
lOFC	0.99	1.00	0.89	0.89
rVLPFC	0.83	0.92	0.74	0.66
lVLPFC	0.87	0.69	0.89	0.59

Table 4. During the VFT period, the AUC for distinguishing UD patients from the other two groups in each prefrontal area, along with the corresponding sensitivity, specificity, and Oxy-Hb cut-off points.

ROC curves were generated for diagnosing healthy controls (HC) across eight cortical regions using fNIRS classification results (Fig. 6). During the VFT task, the right dorsolateral prefrontal cortex (rDLPFC) exhibited the highest area under the curve (AUC) for HC, with an AUC of 0.98. The threshold value was set at 0.83, achieving a sensitivity of 83% and a specificity of 100% (Table 6).
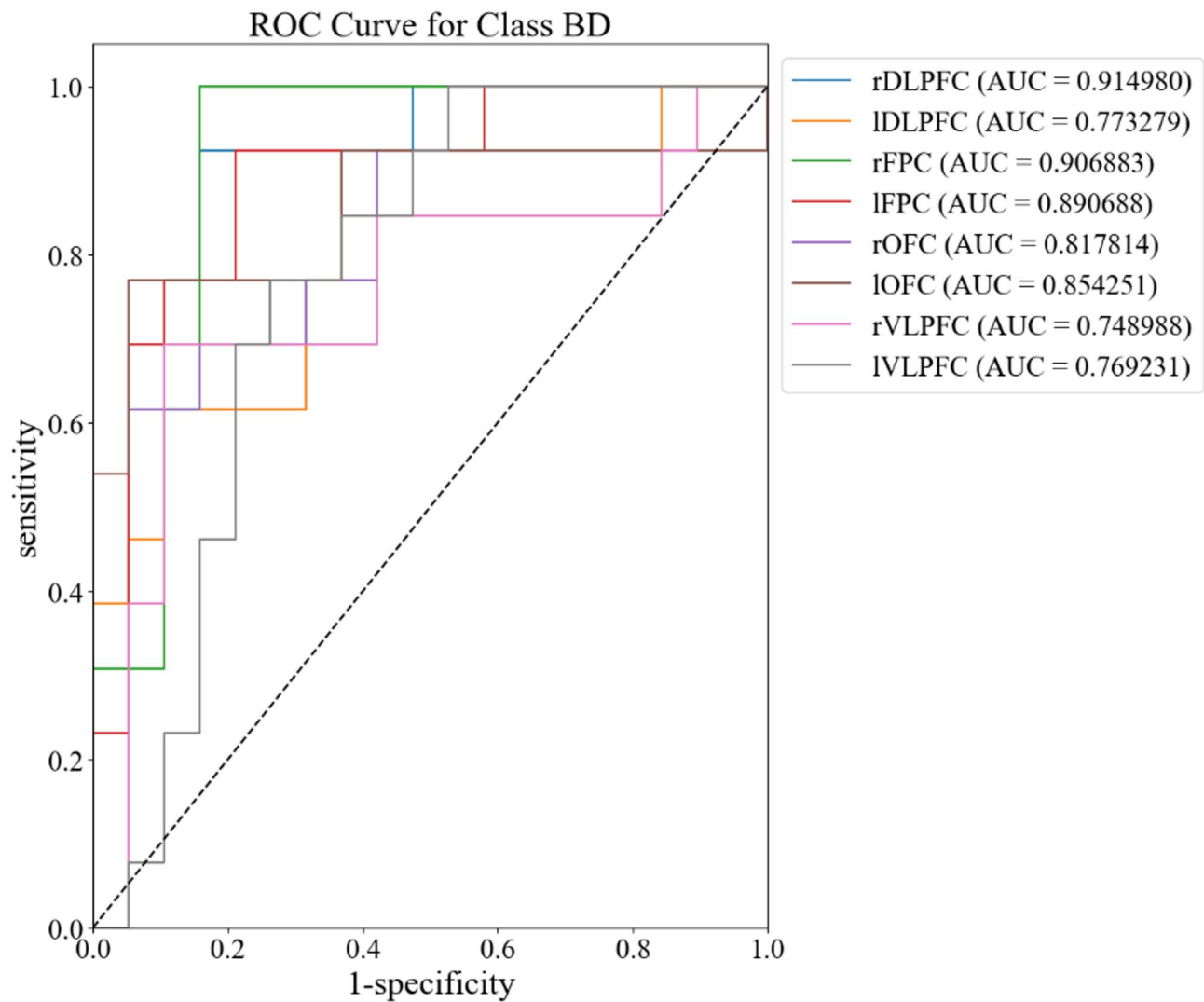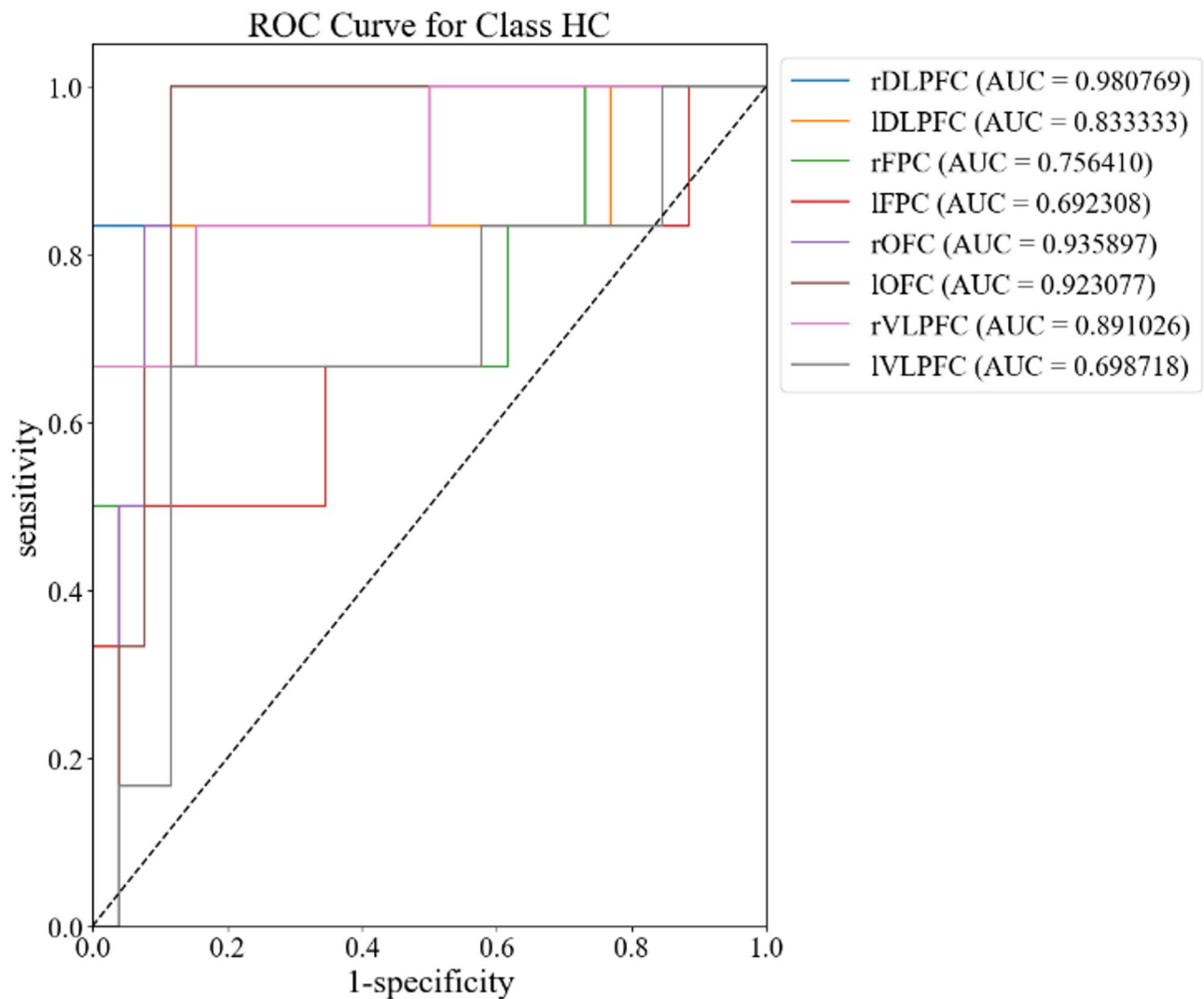
Fig. 5. ROC curve for Class BD.

Region of interest	AUC	Sensitivity	Specificity	Oxy-Hb cut-off point
rDLPFC	0.91	0.78	0.89	0.66
lDLPFC	0.77	0.62	0.89	0.51
rFPC	0.91	1.00	0.79	0.79
lFPC	0.89	0.92	0.79	0.71
rOFC	0.82	0.69	0.84	0.53
lOFC	0.85	0.69	0.89	0.59
rVLPFC	0.75	0.46	0.89	0.36
lVLPFC	0.77	0.85	0.58	0.43

Table 5. During the VFT period, the AUC for distinguishing BD patients from the other two groups in each prefrontal area, along with the corresponding sensitivity, specificity, and Oxy-Hb cut-off points.

Discussion

This study aimed to explore the potential of fNIRS in distinguishing patients with unipolar depression (UD) from those with bipolar disorder (BD). By combining fNIRS and a verbal fluency task (VFT), we assessed differences in prefrontal cortex (PFC) activation patterns across three groups—UD, BD, and healthy controls—using a one-dimensional convolutional neural network (1D-CNN) deep learning approach. Our findings demonstrate distinct PFC activation patterns across the groups during the fNIRS-VFT task, supporting the use of fNIRS as an auxiliary diagnostic tool to improve diagnostic accuracy for UD and BD in clinical settings.

Fig. 6. ROC curve for Class HC.

Region of interest	AUC	Sensitivity	Specificity	Oxy-Hb cut-off point
rDLPFC	0.98	0.83	1.00	0.83
lDLPFC	0.83	0.33	1.00	0.33
rFPC	0.76	0.50	1.00	0.50
lFPC	0.69	0.50	0.96	0.46
rOFC	0.94	0.83	0.88	0.72
lOFC	0.92	0.67	0.92	0.59
rVLPFC	0.89	0.67	0.88	0.55
lVLPFC	0.70	0.17	0.96	0.13

Table 6. During the VFT period, the AUC for distinguishing HC group from the other two groups in each prefrontal area, along with the corresponding sensitivity, specificity, and Oxy-Hb cut-off points.

Our study presents three main findings:

First, both UD and BD patients showed significantly reduced PFC activation compared to healthy participants, consistent with prior research. For example, previous studies using fNIRS reported that BD patients exhibit lower average changes in oxy-Hb during VFTs compared to healthy controls, with reduced bilateral DLPFC activity positively correlated with depression severity[36]. Similar findings have shown that UD patients demonstrate significantly lower oxyhemoglobin levels in both the prefrontal cortex and temporal lobes during VFT tasks relative to healthy participants[15,37,38]. This may be due to the fact that the VFT assesses vocabulary

production, executive ability, and cognitive flexibility[39] and the onset of affective disorders affects mood, and cognition[40] so that patients with affective disorders are imaged differently than healthy individuals on the fNIRS. Prior to the prevalence of fNIRS, studies on magnetic resonance also demonstrated limited activation of brain regions during the Stroop task in patients with bipolar disorder compared to healthy subjects[41] and reduced dynamic functional connectivity between the posterior cingulate cortex and the medial prefrontal cortex in patients with bipolar disorder during the VFT task[42]. Magnetic resonance imaging also revealed an imbalance between left and right prefrontal activation in UD patients during emotion judgments[43] and a decrease in prefrontal activation during the VFT[44]. This may be because glutamate is the main excitatory neurotransmitter in the cerebral cortex that coordinates vascular and metabolic responses to neuronal activity behind changes in functional imaging signals[45]. Patients with mood regulation disorders-bipolar disorder and depression-have elevated levels of glutamate in the frontal cortex, and the frontal glutamatergic system is disturbed thereby affecting brain function[46]. Conversely, prefrontal activation is deficient, the diminution of prefrontal regulation, and the limbic brain is hypothesized to be dysregulated, leading to extreme moods such as mania, depression, and mixed states[47].

Second, UD patients showed notably lower activation values in the DLPFC, FPC, lOFC, and lVLPFC regions compared to BD patients. Both the VLPFC and DLPFC play key roles in emotional regulation[48–50] with the VLPFC particularly involved in the downregulation of negative emotions[51]. Compared to the right VLPFC, feedback from the left VLPFC is associated with enhanced self-regulation capabilities and improved emotional control across the frontal lobe[52]. Increased DLPFC activation has been linked to reduced subjective social distress[53]. The orbitofrontal cortex is functionally connected to brain regions such as the amygdala, hippocampus, and dorsolateral prefrontal lobe, and is responsible for receiving sensory and emotional input signals related to decision-making behaviors[54] reward expectancy[55] impulsivity, and other psychological activities. Reduced OFC function impairs decision-making and emotional processing, and may affect impulsivity in depressed and suicidal individuals[56]. Magnetic coimaging studies of adolescent bipolar depressed patients with suicidal behavior found reduced volume in the left orbitofrontal cortex and that the reduced volume was negatively correlated with suicide-to-mortality rates[57]. The MDD and BD groups had reduced resting-state functional connectivity in the left orbitofrontal cortex and the left anterior cingulate cortex[58]. Orbital frontal cortex-hippocampus (OFC-HPC) circuits were noted to mediate the remission of depression in a study on EEG[59]. The FPC, among the densest cortical regions, is integral to complex social, emotional, and cognitive processes and coordinates DLPFC and VLPFC integration[60,61]. Imaging studies have noted a reduction in grey matter volume in the FPC of UD patients[62]. Kawano found a negative correlation between cerebral blood flow in the FPC and depressive symptom severity, suggesting the FPC as a potential biomarker region for depression severity[63]. Prior studies indicated lower hemodynamic activation in the VLPFC of UD compared to BD patients[15] though these studies often did not distinguish between first-episode and recurrent depression. Other research has noted differences in activation between BD and UD in the left FPC and Broca's area[64]. For instance, Tran's study found that BD patients displayed greater activation in the VLPFC and right FPC than UD patients[65]. Using a VFT paradigm, Liu and colleagues reported activation differences in lateral and orbitofrontal PFC regions between UD and BD patients[66]. The above study partially agrees with our findings, suggesting that bipolar-depressed patients have better activation patterns. For patients with UD and BD there are differences in the performance of brain structures under cognitive tasks may be due to the heterogeneity of mood disorders and the impact of current emotional states on cognitive performance[47]. Although the patients selected for this study were in depressive episodes, patients with BD had more fluctuating mood states throughout the illness, and this heterogeneity may be precisely reflected in the activation patterns[15].

Third, to the best of our knowledge, studies combining MRI and pattern recognition techniques to explore biomarkers of psychiatric disorders have grown substantially in recent years. In a study of resting-state fMRI data from 46 patients with MDD and 57 HCs based on the multivariate pattern analysis (MVPA) learning method, an 86.4% correct classification rate was found[67] and pattern classification analysis using the support vector machine (SVM) method was 86% accurate in distinguishing between BD and UD[68]. BD and UD in an emotional stimulus task with multivariate pattern analysis produced a significant classification rate of 72%[69]. However, these do not involve the training of network structures as complex as deep learning, so we applied a novel deep learning approach using 1D-CNNs to classify fNIRS data, which significantly enhances fNIRS data classification by automatically extracting complex features, thereby improving classification accuracy. Deep neural networks capture nonlinear relationships among brain regions, providing greater robustness and generalizability in multi-class classification tasks. In this study, the three-class classification task achieved an accuracy of 79.57% in the lOFC, a critical region in cognitive processes such as behavioral inhibition, decision-making, and emotional regulation[15,70]. Further analysis revealed that, during the VFT task, the lOFC was the most effective region in diagnosing UD patients, with an AUC of 0.99. Similarly, the rDLPFC demonstrated high diagnostic efficacy for BD patients (AUC = 0.91) and for identifying healthy controls (AUC = 0.98). These findings indicate the high accuracy of our machine learning models in classifying patients with these disorders, underscoring the value and reliability of fNIRS technology as a clinical aid in the diagnosis of psychiatric disorders, and by providing real-time, noninvasive data on neural activity, it can complement the subjective limitations of the DSM-5 and the Structured Interview in terms of both the quantification of biomarkers and the dynamic monitoring of symptoms.

Limitations and future research

Some limitations in this study must be considered. First, the relatively small sample size may have led to an increased risk of confounding and selective bias, so future research needs to test whether these patterns replicate in larger samples. It would have been better to analyze the results by subgroups (gender and age). Although one study found no hemodynamic differences between genders during a verbal working memory task by

fNIRS[71]. And the patients selected for this study were 18–60 years old, although the possible influence of minors and elderly people on the results was avoided, a perfectly matched sample in terms of age and gender is still ideal for subsequent studies, so as to further explore and validate whether this characteristic has an effect on hemodynamics. Second, the patients receiving medications were not ruled out from the study. Although previous studies have revealed no correlation between antidepressant dosages and Oxy-Hb activation in both BD and UD groups[72]. However, further exploration of the confounding effect between the use of multiple medications and changes in brain function is needed. Third, this study was a cross-sectional study. Future longitudinal studies are needed to monitor changes in blood oxygen levels during the disease and the effects of different drugs on hemodynamic activation during the VFT task and to assess the stability of fNIRS-derived biomarkers over time. Fourth, this study did not collect behavioral data from the participants. However, in previous studies, it was found that task performance was not significantly different between many patient and healthy groups[73,74]. Fifth, fNIRS can only measure cortical areas and cannot measure the hemodynamic responses of subcortical structures such as the amygdala. Sixth, the NIRS-KIT toolkit used in this study offers a comprehensive analysis workflow. It also provides flexible data processing capabilities. However, the study did not utilize the Vector Phase Analysis Approach[75]. Omitting this method may hinder the effective separation and analysis of signals related to neural activity, thus affecting the accurate assessment of brain function. Future research could explore and adopt more advanced signal processing techniques to enhance the reliability of the results.

Conclusions

The findings of this study indicate that while both bipolar depression and unipolar depression patients demonstrate significant impairments in emotional regulation compared to healthy controls, patients with bipolar depression retain relatively better emotional regulation abilities than those with unipolar depression. This pattern of differential fNIRS prefrontal-based activation during the processing of cognitive tasks may contribute to elucidating the pathophysiological mechanisms of mood disorders and may serve as a potential marker to help differentiate between bipolar and unipolar depression.

Data availability

The data used to support the findings of this study are available from the corresponding author upon request.

References

1. Goes, F. S. Diagnosis and management of bipolar disorders. *Bmj* **381**, e073591 (2023).
2. Grande, I. et al. Bipolar disorder. *Lancet* **387** (10027), 1561–1572 (2016).
3. Nierenberg, A. A. et al. Diagnosis and treatment of bipolar disorder: A review. *Jama* **330** (14), 1370–1380 (2023).
4. Harrison, P. J., Geddes, J. R. & Tunbridge, E. M. The emerging neurobiology of bipolar disorder. *Trends Neurosci.* **41** (1), 18–30 (2018).
5. Vieta, E. et al. Bipolar disorders. *Nat. Rev. Dis. Primers.* **4**, 18008 (2018).
6. Gao, C. & Li, T. Gender specificity of frontal activity based on fNIRS in distinguishing bipolar depression population from health control. *J. Biophotonics*. **17** (2), e202300346 (2024).
7. Ratheesh, A. et al. A systematic review and meta-analysis of prospective transition from major depression to bipolar disorder. *Acta Psychiatr Scand.* **135** (4), 273–284 (2017).
8. Bai, Y. M. et al. A comparison study of metabolic profiles, immunity, and brain Gray matter volumes between patients with bipolar disorder and depressive disorder. *J. Neuroinflammation.* **17** (1), 42 (2020).
9. Organization, W. H. *International Statistical Classification of Diseases and Related Health Problems (ICD-10).* (1992).
10. Association, A. P. *Diagnostic and Statistical Manual of Mental Disorders: DSM-5* (American Psychiatric Pub, 2013).
11. Yu, Z. et al. Abnormal topology of brain functional networks in unipolar depression and bipolar disorder using optimal graph thresholding. *Prog Neuropsychopharmacol. Biol. Psychiatry.* **96**, 109758 (2020).
12. Andreazza, A. C., Duong, A. & Young, L. T. Bipolar disorder as a mitochondrial disease. *Biol. Psychiatry.* **83** (9), 720–721 (2018).
13. Hare, B. D. & Duman, R. S. Prefrontal cortex circuits in depression and anxiety: contribution of discrete neuronal populations and target regions. *Mol. Psychiatry.* **25** (11), 2742–2758 (2020).
14. Han, K. M. et al. Differentiating between bipolar and unipolar depression in functional and structural MRI studies. *Prog Neuropsychopharmacol. Biol. Psychiatry.* **91**, 20–27 (2019).
15. Feng, K. et al. Differentiating between bipolar and unipolar depression using prefrontal activation patterns: promising results from functional near infrared spectroscopy (fNIRS) findings. *J. Affect. Disord.* **281**, 476–484 (2021).
16. Kim, H. Y. et al. Application of functional Near-Infrared spectroscopy to the study of brain function in humans and animal models. *Mol. Cells.* **40** (8), 523–532 (2017).
17. Husain, S. F. et al. Cortical haemodynamic response during the verbal fluency task in patients with bipolar disorder and borderline personality disorder: a preliminary functional near-infrared spectroscopy study. *BMC Psychiatry.* **21** (1), 201 (2021).
18. Takeda, T. et al. PFC blood oxygenation changes in four different cognitive tasks. *Adv. Exp. Med. Biol.* **977**, 199–204 (2017).
19. Pizzagalli, D. A. & Roberts, A. C. Prefrontal cortex and depression. *Neuropsychopharmacology* **47** (1), 225–246 (2022).
20. Briggs, R. G. et al. Anatomy and white matter connections of the superior frontal gyrus. *Clin. Anat.* **33** (6), 823–832 (2020).
21. Tobiansky, D. J. et al. Androgen regulation of the mesocorticolimbic system and executive function. *Front. Endocrinol. (Lausanne).* **9**, 279 (2018).
22. Rive, M. M. et al. Neural correlates of dysfunctional emotion regulation in major depressive disorder. A systematic review of neuroimaging studies. *Neurosci. Biobehav Rev.* **37** (10 Pt 2), 2529–2553 (2013).
23. Wang, Z. et al. Clinical characteristics and cognitive function in bipolar disorder patients with different onset symptom. *Front. Psychiatry.* **14**, 1253088 (2023).
24. Gyurak, A. et al. Executive functions and the down-regulation and up-regulation of emotion. *Cogn. Emot.* **26** (1), 103–118 (2012).
25. Yeung, M. K. et al. Altered frontal lateralization underlies the category fluency deficits in older adults with mild cognitive impairment: A Near-Infrared spectroscopy study. *Front. Aging Neurosci.* **8**, 59 (2016).
26. Bertola, L. et al. Impaired generation of new subcategories and switching in a semantic verbal fluency test in older adults with mild cognitive impairment. *Front. Aging Neurosci.* **6**, 141 (2014).

27. Ohtani, T. et al. Association between longitudinal changes in prefrontal hemodynamic responses and social adaptation in patients with bipolar disorder and major depressive disorder. *J. Affect. Disord.* **176**, 78–86 (2015).
28. Acharya, U. R. et al. A deep convolutional neural network model to classify heartbeats. *Comput. Biol. Med.* **89**, 389–396 (2017).
29. He, K. et al. Deep Residual Learning for Image Recognition. IEEE, (2016).
30. Wei, Y. Y. et al. Functional near-infrared spectroscopy (fNIRS) as a tool to assist the diagnosis of major psychiatric disorders in a Chinese population. *Eur. Arch. Psychiatry Clin. NeuroSci.* **271** (4), 745–757 (2021).
31. Okada, E. & Delpy, D. T. Near-infrared light propagation in an adult head model. II. Effect of superficial tissue thickness on the sensitivity of the near-infrared spectroscopy signal. *Appl. Opt.* **42** (16), 2915–2922 (2003).
32. Hou, X. et al. NIRS-KIT: a MATLAB toolbox for both resting-state and task fNIRS data analysis. *Neurophotonics* **8** (1), 010802 (2021).
33. Huijun et al. *Near-infrared Spectroscopy for Examination of Prefrontal Activation during Cognitive Tasks in Patients with Major Depressive Disorder: A meta-analysis of Observational Studies* (Psychiatry & Clinical Neurosciences, 2014).
34. Strangman, G., Boas, D. A. & Sutton, J. P. Non-invasive neuroimaging using near-infrared light. *Biol. Psychiatry.* **52** (7), 679–693 (2002).
35. Jalalvandi, M. et al. Brain cortical activation during imagining of the wrist movement using functional Near-Infrared spectroscopy (fNIRS). *J. Biomed. Phys. Eng.* **11** (5), 583–594 (2021).
36. Mao, M. C. et al. Characteristics of prefrontal activity during emotional and cognitive processing in patients with bipolar disorder: A multi-channel functional near-infrared spectroscopy study. *Front. NeuroSci.* **16**, 946543 (2022).
37. Ho, C. S. H. et al. Diagnostic and predictive applications of functional Near-Infrared spectroscopy for major depressive disorder: A systematic review. *Front. Psychiatry.* **11**, 378 (2020).
38. Ong, S. K. et al. Integration of the cortical haemodynamic response measured by functional Near-Infrared spectroscopy and amino acid analysis to aid in the diagnosis of major depressive disorder. *Diagnostics (Basel)* **11**(11), 1978 (2021).
39. Herrmann, M. J. et al. Relevance of dorsolateral and frontotemporal cortex on the phonemic verbal Fluency - A fNIRS-Study. *Neuroscience* **367**, 169–177 (2017).
40. Schneider, M. R. et al. Neuroprogression in bipolar disorder. *Bipolar Disord.* **14** (4), 356–374 (2012).
41. Strakowski, S. M. et al. Abnormal FMRI brain activation in euthymic bipolar disorder patients during a counting Stroop interference task. *Am. J. Psychiatry.* **162** (9), 1697–1705 (2005).
42. Liang, Y. et al. Disturbances of dynamic function in patients with bipolar disorder I and its relationship with Executive-Function deficit. *Front. Psychiatry.* **11**, 537981 (2020).
43. Grimm, S. et al. Imbalance between left and right dorsolateral prefrontal cortex in major depression is linked to negative emotional judgment: an fMRI study in severe major depressive disorder. *Biol. Psychiatry.* **63** (4), 369–376 (2008).
44. Okada, G. et al. Attenuated prefrontal activation during a verbal fluency task in remitted major depression. *Psychiatry Clin. Neurosci.* **63** (3), 423–425 (2009).
45. Duncan, N. W. et al. Involvement of glutamate in rest-stimulus interaction between perigenual and supragenual anterior cingulate cortex: a combined fMRI-MRS study. *Hum. Brain Mapp.* **32** (12), 2172–2182 (2011).
46. Hashimoto, K., Sawa, A. & Iyo, M. Increased levels of glutamate in brains from patients with mood disorders. *Biol. Psychiatry.* **62** (11), 1310–1316 (2007).
47. Strakowski, S. M. et al. The functional neuroanatomy of bipolar disorder: a consensus model. *Bipolar Disord.* **14** (4), 313–325 (2012).
48. Buhle, J. T. et al. Cognitive reappraisal of emotion: A Meta-Analysis of human neuroimaging studies. *Cereb. Cortex* **24**(11), 2981–2990 (2014).
49. He, Z. et al. Critical role of the right VLPFC in emotional regulation of social exclusion: a tDCS study. *Soc. Cogn.Affect. Neurosci.* **13**(4), 357–366 (2018).
50. Kohn, N. et al. Neural network of cognitive emotion regulation–an ALE meta-analysis and MACM analysis. *Neuroimage* **87**, 345–355 (2014).
51. He, Z. et al. The VLPFC-Engaged voluntary emotion regulation: combined TMS-fMRI evidence for the neural circuit of cognitive reappraisal. *J. Neurosci.* **43** (34), 6046–6060 (2023).
52. Keller, M. et al. fMRI Neurofeedback-Enhanced cognitive reappraisal training in depression: A Double-Blind comparison of left and right VlPFC regulation. *Front. Psychiatry.* **12**, 715898 (2021).
53. Koban, L. et al. Frontal-Brainstem pathways mediating placebo effects on social rejection. *J. Neurosci.* **37** (13), 3621–3631 (2017).
54. Banerjee, A. et al. Value-guided remapping of sensory cortex by lateral orbitofrontal cortex. *Nature* **585** (7824), 245–250 (2020).
55. Howard, J. D. et al. Targeted stimulation of human orbitofrontal networks disrupts Outcome-Guided behavior. *Curr. Biol.* **30** (3), 490–498e4 (2020).
56. Zanghì, E., Corallo, F., Lo, V. & Buono Diffusion tensor imaging studies on subjects with suicidal thoughts and behaviors: A descriptive literature review. *Brain Behav.* **12** (9), e2711 (2022).
57. Huber, R. S. et al. Reduced lateral orbitofrontal cortex volume and suicide behavior in youth with bipolar disorder. *Bipolar Disord.* **21** (4), 321–329 (2019).
58. Chen, L. et al. Common and distinct abnormal frontal-limbic system structural and functional patterns in patients with major depression and bipolar disorder. *Neuroimage Clin.* **20**, 42–50 (2018).
59. Han, S. et al. Orbitofrontal cortex-hippocampus potentiation mediates relief for depression: A randomized double-blind trial and TMS-EEG study. *Cell. Rep. Med.* **4** (6), 101060 (2023).
60. Wu, H. et al. Differences in prefrontal cortex activation in Chinese college students with different severities of depressive symptoms: A large sample of functional near-infrared spectroscopy (fNIRS) findings. *J. Affect. Disord.* **350**, 521–530 (2024).
61. Shimoda, K. et al. Activation of the prefrontal cortex while performing a task at preferred slow Pace and metronome slow Pace: a functional near-infrared spectroscopy study. *Neural Plast.* **2014**, p269120 (2014).
62. Amidfar, M. et al. Grey matter volume abnormalities in the first depressive episode of medication-naïve adult individuals: a systematic review of voxel based morphometric studies. *Int. J. Psychiatry Clin. Pract.* **25** (4), 407–420 (2021).
63. Kawano, M. et al. Correlation between frontal lobe oxy-hemoglobin and severity of depression assessed using near-infrared spectroscopy. *J. Affect. Disord.* **205**, 154–158 (2016).
64. Zhu, Y. et al. Prefrontal activation during a working memory task differs between patients with unipolar and bipolar depression: A preliminary exploratory study. *J. Affect. Disord.* **225**, 64–70 (2018).
65. Tran, B. X. et al. Utility of portable functional near-infrared spectroscopy (fNIRS) in patients with bipolar and unipolar disorders: A comparison with healthy controls. *J. Affect. Disord.* **323**, 581–591 (2023).
66. Liu Xiaomin, L. P., Chen & Guifang Feng kun, the different activation patterns of the prefrontal cortex between bipolar depression and unipolar depression under voice fluency task. *Chin. J. Psychiatry.* **55** (03), 182–188 (2022).
67. Zhong, X. et al. Whole-brain resting-state functional connectivity identified major depressive disorder: A multivariate pattern analysis in two independent samples. *J. Affect. Disord.* **218**, 346–352 (2017).
68. Li, M. et al. Clinical utility of a short resting-state MRI scan in differentiating bipolar from unipolar depression. *Acta Psychiatr Scand.* **136** (3), 288–299 (2017).
69. Bürger, C. et al. Differential abnormal pattern of anterior cingulate gyrus activation in unipolar and bipolar depression: an fMRI and pattern classification approach. *Neuropsychopharmacology* **42** (7), 1399–1408 (2017).

12

70. Jones, D. T. & Graff-Radford, J. Executive dysfunction and the prefrontal cortex. *Continuum (Minneap Minn)*. **27** (6), 1586–1601 (2021).
71. Li, T., Luo, Q. & Gong, H. Gender-specific hemodynamics in prefrontal cortex during a verbal working memory task by near-infrared spectroscopy. *Behav. Brain Res.* **209** (1), 148–153 (2010).
72. Nishimura, Y. et al. Social function and frontopolar activation during a cognitive task in patients with bipolar disorder. *Neuropsychobiology* **72** (2), 81–90 (2015).
73. Takamura, M. et al. Disrupted brain activation and deactivation pattern during semantic verbal fluency task in patients with major depression. *Neuropsychobiology* **74** (2), 69–77 (2016).
74. Tomioka, H. et al. A longitudinal functional neuroimaging study in medication-naïve depression after antidepressant treatment. *PLoS One.* **10** (3), e0120828 (2015).
75. Lim, L. G. et al. Optimizing mental workload Estimation by detecting baseline state using vector phase analysis approach. *IEEE Trans. Neural Syst. Rehabil Eng.* **29**, 597–606 (2021).

Author contributions

L.M.,Y.S.and Z.S.:Study concept and design. Q.T.and X.Z.:Data collection. B.W.and J.Z.:Statistical analysis of data.L.M.: Manuscript preparation.Z.W.,C.Z.,Y.S.and Z.S: Critical revision of the manuscript. All authors contributed to the article and approved the submitted version.

Funding

Declarations

Competing interests

The authors declare no competing interests.

Ethics statement

This study is conducted in accordance with the latest version of the Declaration of Helsinki and is approved by the Huzhou Third Municipal Hospital Institutional Review Board(the approval number: [2023 − 480]). The patients/participants provided their written informed consent to participate in this study. Written informed consent was obtained from the individual(s) for the publication of any potentially identifiable images or data included in this article.

Additional information

Correspondence and requests for materials should be addressed to Z.S.

Reprints and permissions information is available at www.nature.com/reprints.

Publisher's note Springer Nature remains neutral with regard to jurisdictional claims in published maps and institutional affiliations.